Implementation of an IBBCEAS technique in an atmospheric simulation chamber for *in situ* NO$_3$ monitoring: characterization and validation for kinetic studies

Axel Fouqueau[1], Manuela Cirtog[1], Mathieu Cazaunau[1], Edouard Pangui[1], Pascal Zapf[1], Guillaume Siour[1], Xavier Landsheere[1], Guillaume Méjean[2], Daniele Romanini[2], Bénédicte Picquet-Varrault[1]

[1]LISA, UMR CNRS 7583, Université Paris-Est Créteil, Université de Paris, Institut Pierre Simon Laplace (IPSL), Créteil, France

[2]LIPHY, UMR CNRS 5588, Université Grenoble Alpes, Grenoble, France

Correspondence to: Manuela Cirtog (manuela.cirtog@lisa.u-pec.fr)

Abstract. An incoherent broadband cavity-enhanced absorption spectroscopy (IBBCEAS) technique has been developed for *in situ* monitoring of NO$_3$ radicals at the ppt level in the CSA simulation chamber (at LISA). The technique couples an incoherent broadband light source centered at 662 nm with a high finesse optical cavity made of two highly reflecting mirrors. The optical cavity which has an effective length of 82 cm allows for up to 3 km of effective absorption and a high sensitivity for NO$_3$ detection (up to 6 ppt for an integration time of 10 seconds). This technique also allows NO$_2$ monitoring (up to 9 ppb for an integration time of 10 seconds). Here, we present the experimental setup as well as tests for its characterization and validation. The validation tests include an intercomparison with another independent technique (FTIR) and the absolute rate determination for the reaction *trans*-2-butene + NO$_3$ which is already well documented in the literature. The value of $(4.13 \pm 0.45) \times 10^{-13}$ cm^3 molecule^{-1} s^{-1} has been found, which is in good agreement with previous determinations. From these experiments, optimal operation conditions are proposed. The technique is now fully operational and can be used to determine rate constants for fast reactions involving complex volatile organic compounds (with rate constants up to 10^{-10} cm^3 molecule^{-1} s^{-1}).

1. Introduction

The night time chemistry in polluted urban or sub-urban areas has been proved to be governed by NO$_3$ radicals since its discovery in the 1980s *(Naudet et al., 1981; Noxon et al., 1978, 1980; Platt et al., 1980)*. In particular, the NO$_3$ radical has been shown to be an efficient oxidant for some organic compounds, or in some cases even the dominant one, thus impacting the budget of these species and their degradation products. Unsaturated VOCs, including biogenic VOCs, are particularly reactive towards NO$_3$ radicals *(Wayne et al., 1991)*. Providing kinetic data for these reactions is essential for a better understanding of the role of NO$_3$ radicals in their degradation. Nevertheless, due to the high reactivity of some unsaturated VOCs with NO$_3$ (with rate constants which can reach 10^{-11} to 10^{-10} cm^3 molecule^{-1} s^{-1}), absolute rate determination for these reactions appears to be difficult as it requires the use of a highly sensitive method for NO$_3$ monitoring. As a consequence, the number of absolute kinetic studies for the NO$_3$-initiated oxidation of terpenes is very limited and this leads to large uncertainties on this chemistry as it has been pointed out in the literature *(Atkinson, 2000; Brown and Stutz, 2012; Ng et al., 2017)*. *Calvert et al., 2015* gave recommendations for NO$_3$ oxidation rate constants for 91 alkenes (ranging between 10^{-16} and 10^{-10} cm^3 molecule^{-1} s^{-1}) and more than 98 % of the determinations on which these recommendations are based were conducted using the relative rate method. One of the reasons for this is still the challenging measurement of NO$_3$

radicals at low mixing ratios (<100 ppt) during such experiments. For these compounds, new absolute
determinations are essential to better evaluate the role of NO_3 radical in their degradation.

Among the various experimental tools which are currently used to measure rate constants, atmospheric simulation chambers represent suitable tools for performing experiments under very realistic atmospheric conditions. This implies low concentrations of reactants in order to minimize possible secondary reactions. Another benefit of these facilities is the high analytical capabilities which allow *in situ* monitoring of reactants and products with a high sensitivity. Even though significant progress has been made in the last decades for NO_3 radicals measurement at low concentrations with the arising of cavity enhanced and cavity ring down spectroscopic techniques (Ball et al., 2004; Bitter et al., 2005; Kennedy et al., 2011; Langridge et al., 2008) as well as laser induced fluorescence techniques (Matsumoto et al., 2005b, 2005c, 2005a; Wood et al., 2003), it is observed only few were coupled to simulation chambers (Dorn et al., 2013; Venables et al., 2006; Wu et al., 2014).In addition, to our knowledge, none of these techniques has been used for kinetic applications involving NO_3 radical in simulation chambers.

For this purpose, the analytical capabilities of the CSA chamber available at LISA have been improved by developing a sensitive technique for measuring NO_3 radicals at very low concentration. An incoherent broadband cavity enhanced absorption spectroscopy (IBBCEAS) technique has been coupled to the chamber with the objective of performing high sensitivity *in situ* NO_3 monitoring with integration time of seconds.

In this paper, we describe the experimental setup and the characterization of the technique. Finally, the IBBCEAS technique has been validated thanks to an intercomparison of NO_2 and NO_3 measurement with FTIR technique and an absolute rate determination for the well-known reaction *trans*-2-butene+NO_3.

2. Experimental section

2.1. The CSA chamber

The CSA chamber is made of a large and evacuable Pyrex® reactor (6 m length, 45 cm diameter and 977 L volume) which has been previously presented in detail (Doussin et al., 1997). It is equipped with a homogenization system which is made of i) an injection pipe (4 meters long, 1 cm diameter and regularly drilled with 1 mm holes) which allows to inject the reactants all along the chamber, ii) 2 stainless steel fans allowing a homogenization of gas inside the chamber and iii) a close-circuit Teflon pump connected at both ends allowing a recirculation of the gas mixing. This system allows a mixing time below one minute. The chamber is also equipped with two *in situ* spectroscopic analytical devices coupled with "White" type multiple reflection systems inside the reactor: (i) a FTIR spectrometer (Bruker Vertex 80) which allows acquiring spectra in the range of 600-4000 cm^{-1} with a maximal spectral resolution of 0.07 cm^{-1} and an optical path length of 204 m; (ii) an UV-Visible grating spectrometer consisting of a high-pressure Xenon arc lamp (Osram XBO, 450 W Xe UV), a monochromator HR 320 (Jobin-Yvon) and a CCD camera (CCD 3000, 1024 x 58 pixel, Jobin-Yvon) as a detector. This spectrometer allows acquiring spectra with a spectral resolution of 0.18 nm and an optical path length of 72 m.

This facility has intensively been used to investigate complex gas-phase chemistry involving organic compounds and to provide kinetic and mechanistic data. In particular, it has been used for absolute rate determination of reactions involving NO_3 radicals with a series of VOCs like ethers, esters and aldehydes (Kerdouci et al., 2012; Picquet-Varrault et al., 2009; Scarfogliero et al., 2006). In these studies, NO_3 was monitored at 662 nm with the *in situ* UV-visible spectrometer. However, due to the poor detection limit (0.5 ppb for 1 minute of acquisition),

and taking into account the experimental conditions, the range of rate constants that can be investigated is limited ($< 10^{-12}$ cm^3 molecule^{-1} s^{-1}) preventing from studying very reactive chemical systems, such as BVOC+NO$_3$ reactions.

80 ## 2.2. The IBBCEAS setup

In order to improve the analytical capabilities of the CSA chamber, an IBBCEAS has been developed and coupled to the chamber for high sensitivity *in situ* NO$_3$ monitoring. A detailed description of the technique has been provided in previous works (Langridge et al., 2008; Romanini et al., 1997). IBBCEAS measurements are conducted by exciting with an incoherent broad-band source, a high finesse optical cavity formed by two mirrors

85 with high reflectivity (R(λ) ~99.98 %). Photons resonate between the two mirrors increasing their lifetime in the cavity by a factor of $1/(1-R(\lambda))$. During this time, photons traverse an effective path length of kilometers inside the cavity making possible observations of absorbing species at very low concentrations. The intensity transmitted by the optical cavity rapidly reaches steady state. The optical intracavity absorption coefficient of the sample $\alpha(\lambda)$ can then be calculated with the following expression if accurate measurement of cavity reflectivity R(λ) and

90 of the distance between the mirrors (d) is provided (Engel et al., 1998):

$$\alpha(\lambda) = (\frac{I_0(\lambda)}{I(\lambda)} - 1)(\frac{1-R(\lambda)}{d}) \tag{Eq. 1}$$

Here I(λ) and I$_0$(λ) are the transmitted intensities measured in the presence and in absence of the absorbing species respectively.

The concentrations of the absorbing molecules can then be calculated using a least square algorithm to

95 simultaneously fit the molecules absorption cross section using the formula:

$$\alpha(\lambda) = \sum_i [X_i]\, \sigma_{X_i}(\lambda) + p(\lambda) \tag{Eq. 2}$$

Where, $\sigma_{X_i}(\lambda)$ are the absorption cross sections, [X] are the species absorbing in the considered spectral region and p(λ) is a cubic polynomial to correct baseline deformations due to potential variations of the source intensity (Venables et al., 2006) or to absorption and/or scattering of particles in the chamber (Varma et al., 2013).

100 The optical cavity is made of two high reflectivity mirrors (Layertec, planar/concave mirrors with a 1 m radius of curvature, nominal reflectivity of 99.98 $\pm$ 0.01 % between 630 and 690 nm). It has been transversally installed on the CSA chamber using two co-axial outputs of the reactor. A scheme of the IBBCEAS instrument interfaced to the chamber is shown in Fig. 1. The distance between the mirrors is 82 cm and includes 45 cm for the chamber diameter, 2 $\times$ 10.5 cm for the Pyrex outputs and 2 $\times$ 8 cm for the interface mounts between the chamber and the

105 commercial CRD Optics mount support. In order to prevent adsorption of semi-volatile species or deposition of particles on the mirrors, which would result in a significant decrease of the reflectivity, the mirrors can be protected thanks to a continuous nitrogen flush (flow rate: 300 mL min^{-1}) using a 1/16 inch input disposed close to the mirror surface. This flow rate has been optimized in order to efficiently protect the mirrors while limiting the dilution of the mixture in the measurement area. By comparing the absorption coefficients measured with and without the

110 flush, for a known quantity of NO$_2$ in the chamber, this effective length was estimated to be d$_{eff}$ = 62 $\pm$ 3 cm (i.e. 24% lower than the physical length of the cavity). Nitrogen flush was not used in this study, but is available for

further type of experiments. Thanks to the mixing system which ensures a fast homogenization of the mixture in the chamber, this effective length was observed to be constant during the whole duration of an experiment.
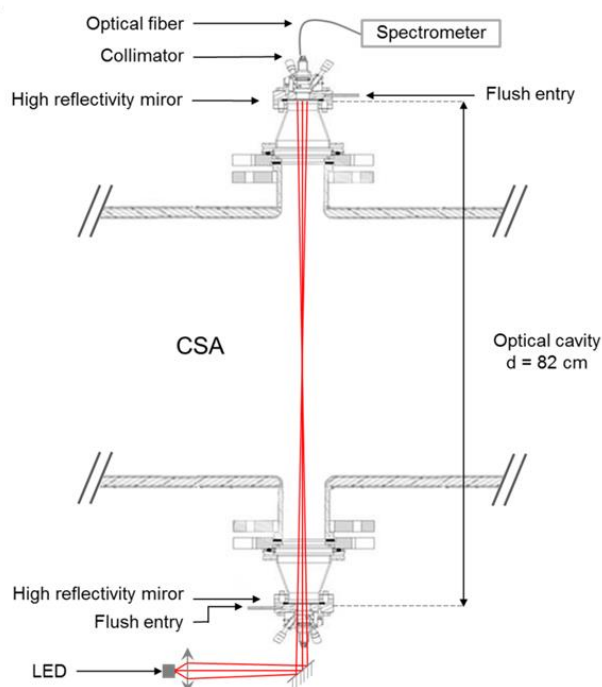
   Figure 1 : Scheme (transverse section) of the IBBCEAS instrument interfaced to the CSA chamber. Collimating lenses and curved mirrors are not shown on the beam injection side.

A light emitting diode (LED, Mouser Electronics – Starboard, Luminus SST-10-DR-B130 DEEp Red, K, max. 430 mW, D5) with an approximative Gaussian shaped emission of 19 nm full width at half maximum (FWHM) and centered at 662 nm was used in order to monitor NO_3 at its maximum absorption wavelength. The LED

   emission spectrum is compared to the cross section spectra of NO_3 (Orphal et al., 2003) and NO_2 (Vandaele et al., 1997) in Fig. 2. The spectral range of the LED is large enough to allow monitoring both NO_2 and NO_3.
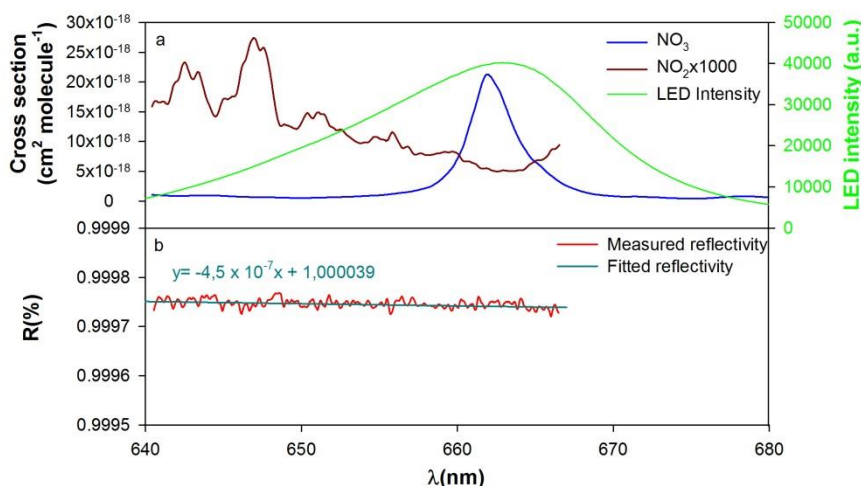
Figure 2: (a) NO₃ and NO₂ absorption cross sections *(Orphal et al., 2003; Vandaele et al., 1997)* between 640 and 680 nm (convolved with apparatus function of the spectrometer) and LED emission spectrum and (b) mirror reflectivity

The LED is mounted on a thermo electric controller (TEC) device (ThermoElectric Cooling, Laser Mount Arroyo Instruments) to ensure a very precise temperature regulation (± 0.01 °C) and stabilize the spectral distribution of the LED. With this device, changes in the LED intensity have been observed to be below 0.3 %. A laser diode controller (Arroyo Instrument 6310) provides the electric power for both TEC and LED (LED current is fixed at 900 mA). Light emitted by the LED is spatially incoherent and collimation is required for an effective coupling with the optical cavity. The light is hence focused with a convex lens (Thorlabs Aspheric Condenser Lens, 25.4 mm diameter, F = 16 mm, NA = 0.79) and injected into the optical cavity with two concave mirrors (Thorlabs, protected silver, diameter 50.8 mm, f = 50mm and diameter 75 mm, f = 500 mm respectively) in order to focus the beam in the middle of the cavity. Light transmitted through the cavity is directed thanks to a collimator (Thorlabs SMA Fiber Collimation Pkg, 635 nm, f = 35.41 mm, NA = 0.25) and an optical fiber (Ocean Optics VIS-NIR (200 μm slit, 5m long) to a miniature Ocean Optics QE65000 spectrometer. The spectrometer measures the cavity output wavelength dependent intensity and comprises a spectrograph interfaced to a charged coupled device (CCD) thermally stabilized at -15°C to minimize dark current. The spectral range covered by the spectrometer is 45 nm (640-685 nm) with a spectral resolution of 0.2 nm. In order to calculate the concentrations of absorbing species, a data treatment program has been developed in R (Ihaka and Gentleman, 1996) using a least square algorithm. A third-degree polynomial function is used in the fit to take into account baseline deformation due to small changes in the source intensity. The concentrations of the absorbing species and the polynomial function are fitted by minimizing the RMSE (root mean square error). In practice, the optimization was run following a bound optimization by quadratic approximation (BObyQA) method (Powell, 2009). The iterative process to minimize the RMSE (between absorption coefficients from Eq. 1 and Eq.2) stops when none of the parameters vary more than 0.2 % between two successive iterations. In the studied spectral range, absorbing species are H₂O, NO₂ and NO₃. Absorption by water vapor may be very high under atmospheric conditions. Nevertheless, due to dry conditions used during the experiments (RH < 1 %), H₂O absorption was negligible here. The absorption cross sections used are provided by the literature (Orphal et al., 2003; Vandaele et al., 1997) and have been convoluted with the apparatus function of the instrument. Because NO₂ cross sections provided by Vandaele et al., 1997 are measured up to 666.5 nm, the treatment has systematically been conducted up to this

value. The cross sections used for the data treatment are presented in Fig. 2**Erreur ! Source du renvoi introuvable.**.

3. Technique qualification and characterization

155   Several experiments have been carried out to assess the stability, the accuracy and the detection limit of the technique. First experiments have been conducted to test the optical stability and the influence of pressure variations on the device. These tests have shown that the instrument is very stable (variations < 1 %). Two aspects have been shown to be particularly critical for measurement with IBBCEAS technique: I_0 measurement and the determination of mirror reflectivity.

3.1. Determination of the cavity reflectivity

160   Having a precise knowledge of the wavelength dependent mirror reflectivity, $R(\lambda)$, is one of the most critical point of the IBBCEAS technique (Venables et al., 2006). Two different methods have been proposed for accurate determination of $R(\lambda)$: i) measurement of a known concentration of an absorbing species (Ventrillard-Courtillot et al., 2010), ii) measurement of the ring-down time in the empty cavity using a pulsed laser CRDS technique (Ball

165 et al., 2004). The first method has been employed here. The absorbing species which has been chosen for the experiments is NO_2 as it absorbs in the whole spectral region of the LED emission and its absorption cross sections are known with high accuracy. NO_2 concentrations in the simulation chamber were obtained from *in situ* FTIR measurements using IBI_{NO2} (1530–1680 cm^{-1}) = $(5.6 \pm 0.2) \times 10^{-17}$ cm molecule^{-1} (base e,). To retrieve the mirror reflectivity $R(\lambda)$ from NO_2 concentration, the following equation is used:

170   $$R(\lambda) = 1 - d \times \sigma_{NO_2}(\lambda) \times [NO_2] \times \left(\frac{I_0(\lambda)}{I(\lambda)} - 1\right)^{-1}$$ (Eq. 3)

where $\sigma_{NO_2}(\lambda)$ is the NO_2 absorption cross section (Vandaele et al., 1997) and [NO$_2$] is the concentration of NO_2 determined by FTIR. In order to reduce the uncertainty on the reflectivity determination and to compensate the weak cross sections of NO_2 in the 660–670 nm region, high concentrations (up to 800 ppb) were used. A plot showing the variation of the reflectivity in function of the wavelength is presented as an example in Fig. 2**Erreur !**

175 **Source du renvoi introuvable.**. Due to the NO_2 reference spectrum, the reflectivity is measured up to 666.5 nm. During this experiment, the reflectivity was observed to vary between 99.975 at 640 nm and 99.974 % at 667 nm and this is in agreement with the reflectivity provided by the supplier (99.98 $\pm$ 0.01 %). It was found to have a slight dependence with wavelengths ($y = -4.5 \times 10^{-7}x + 1.000039$), which justifies that it is necessary to measure it on a wide wavelengths range. At 662 nm, which corresponds to the maximum of NO_3 absorption, the

180 reflectivity was found to be 99.974 %. At this wavelength, the effective absorption path length estimated from Eq. 4 is found to be 3.15 km:

$$X(\lambda) = d/\left(1 - R(\lambda)\right)$$ (Eq. 4)

In addition, it has been observed that the reflectivity of the cavity can significantly vary with the mirror cleanliness. As an example, successive experiments showed that reflectivity can vary at 662 nm from 99.974 % to 99.971 %

185 from one experiment to another, leading to variations of the effective absorption path length of almost 12 %. Therefore, it is crucial to precisely determine the reflectivity prior to each experiment.

3.2. $I_0(\lambda)$ measurement

Previous studies (Fuchs et al., 2010; Kennedy et al., 2011; Ventrillard-Courtillot et al., 2010) have pointed out that the $I_0(\lambda)$ has to be periodically recorded during an experiment to ensure accurate measurement with the IBBCEAS technique. Indeed, changes in the lamp emission spectrum or poor optical stability may induce changes in the absorption coefficient and therefore generate errors in the quantification of the species. This fact may be an issue for experiments in simulation chambers as the $I_0(\lambda)$ can only be recorded before injecting the reactants and experiments can then last for several hours.

In order to evaluate the stability of the signal during a typical experiment and the uncertainty generated by the use of a unique $I_0(\lambda)$ on the quantification of the species, two types of experiments have been performed: first, the stability of the optical system has been verified. For this purpose, long term measurements of the signal have been performed, leading to variations lower than 0.3% and to very small baseline distortions. Then, to verify the impact of these variations on the quantification of absorbing species, experiments were conducted by injecting NO_2, which was observed to be stable in the chamber, and by monitoring its concentration with the IBBCEAS technique for several hours: after the chamber has been filled with a mixture of N_2/O_2 (80/20) at atmospheric pressure, the $I_0(\lambda)$ has been measured. Then, a concentration of NO_2 was introduced into the chamber (mixing ratios ranging between 100 ppb and 1 ppm, depending of the experiment) and the signal $I(\lambda)$ was measured. From these measurements, the absorption coefficient and the NO_2 concentration have been calculated and plotted as a function of time in Fig. 3**Erreur ! Source du renvoi introuvable.**, for a concentration of 1 ppm of NO_2. An increase up to 3 % in NO_2 concentration has been observed 2 hours after recording the $I_0(\lambda)$ due to the deviation of the baseline which is no longer well corrected by the polynomial function. These results suggest that the accuracy of the measurement is significantly reduced after 2 hours. The length of the experiments should therefore not exceed this duration. Above this limit the uncertainty due to a unique measurement of the $I_0(\lambda)$ can be considered as negligible.
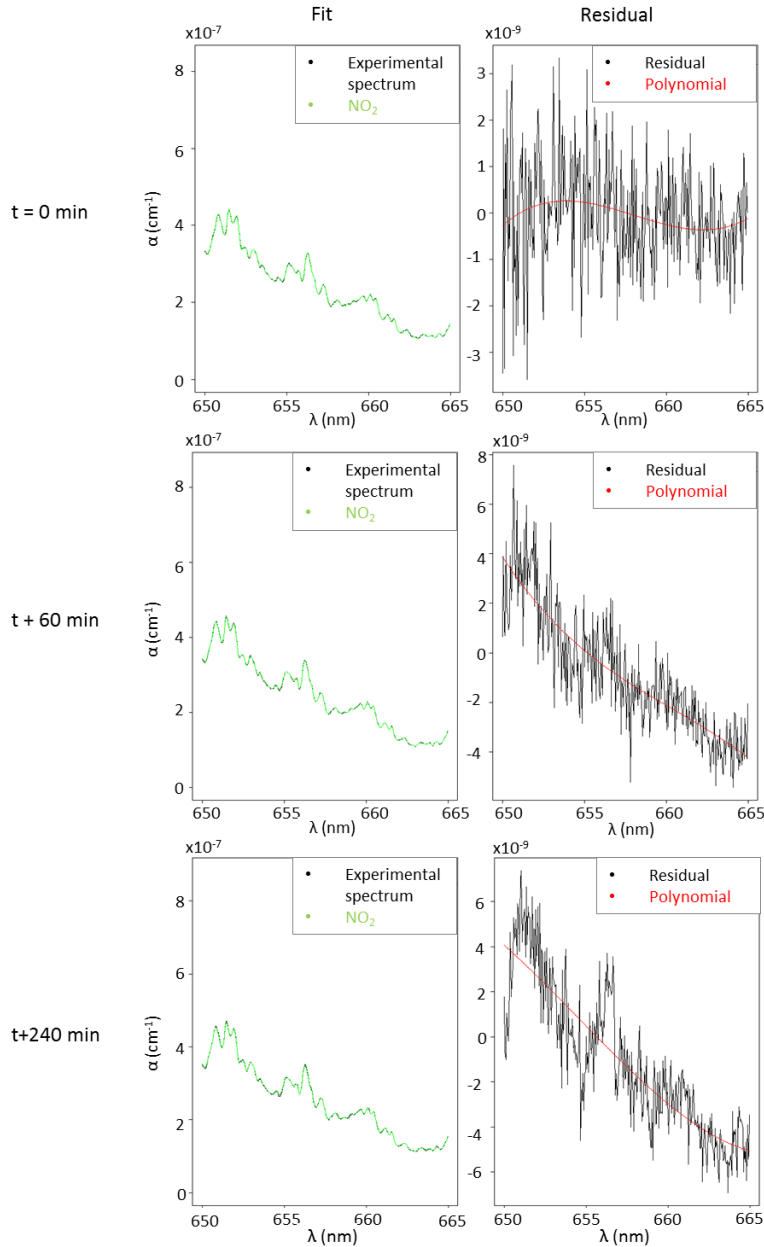
Figure 3 : Evolution of fit quality as a function of time since I_0 was made, measured for 1 ppm of NO_2

3.3. Detection limit and Allan variance

The detection limit for NO_3 radical was estimated by considering 3 times the peak-to-peak noise on the absorption coefficient at 662 nm, which corresponds to the maximum absorption of NO_3 radical. For 10 seconds of acquisition time (which corresponds to 25 acquisitions of 400 ms) and an unpurged system, it has been found to be 1.2×10^{-9} cm^{-1}. Considering that NO_3 radical cross section at this wavelength is 2.2×10^{-17} cm^2 $molecule^{-1}$, the detection limit for NO_3 was estimated to 6 ppt. The same approach was used to estimate the detection limit for NO_2. Between 645 and 650 nm, which correspond to the two main absorption peaks of NO_2, noise has been found to be 2×10^{-9} cm^{-1}. Considering the difference of maximum and minimum absorption of 2.2×10^{-20} cm^2 $molecule^{-1}$ in this range, detection limit has been found to be 11 ppb for 10s of integration time. A spectrum measured with an acquisition

time of 10 s, for 6 ppt of NO_3 and 630 ppb of NO_2 is shown for illustration in Fig. 4**Erreur ! Source du renvoi introuvable.**. The used fit range was between 655 and 666.5 nm. Even at this low level of NO_3 concentration, the absorption is clear and allows its quantification. The fit appears to be satisfying for both NO_2 and NO_3 and the

225   residual spectrum appears to be essentially made of noise, showing a good efficiency of the polynomial fit and a satisfying subtraction of species contributions. This figure shows that this wavelength range is efficient for a precise detection and quantification of both species and validates the detection limit.
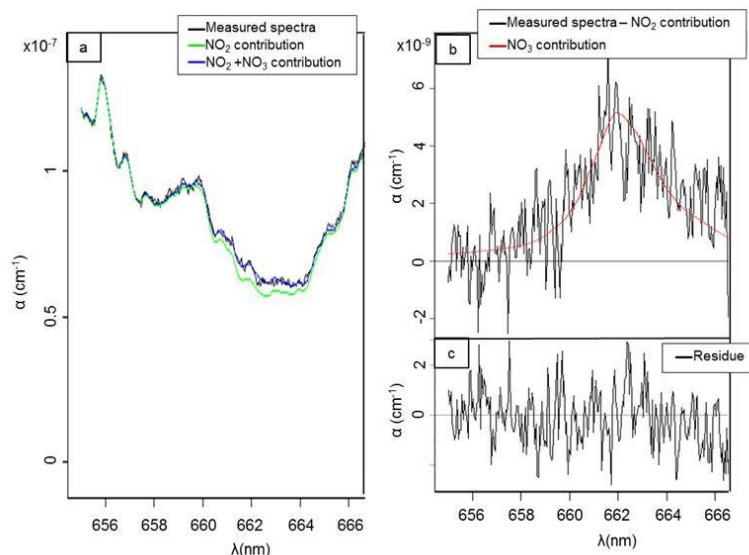
Figure 4: (a) measured absorption coefficient α(λ) (between 655 and 669 nm) with integration time of 10 s (in black);
230   **complete fit of NO_2 and NO_3 (in blue) with [NO_3] = 6 ppt; [NO_2] = 630 ppb; NO_2 fit only (in green) ; (b) measured absorption coefficient (in black) without NO_2 contribution and fitted with [NO_3] = 6 ppt (in red); (c) residue of measured and fitted absorption coefficient.**

The potential of the IBBCEAS technique for measuring NO_3 radical during simulation chamber experiments has already been explored in previous works. It has been coupled to the simulation chamber at UCC (Cork, Ireland),

235   to SAPHIR chamber at FZJ, (Jülich, Germany) and to CHARME chamber at LPCA (Wimereux, France). The characteristics and performances of the various instruments are compared in Table 1**Erreur ! Source du renvoi introuvable.**. Our instrument exhibits very good performances with detection limit similar to those of the other instruments, but for shorter integration time and/or for smaller effective length. This reflects the very good stability of the optical system. These results also prove the potential of this technique for measuring NO_3 radical at low

240   level of concentrations with a good time resolution (10 s) and thus suitable for kinetic measurements.

Table 1 : Comparison of characteristics and performances of various IBBCEAS coupled to simulation chambers for the detection of NO₃ radicals.

In situ IBBCEAS	Deff* (cm)	DL / Integration time	Reference
LISA, Créteil France	**82**	**6 ppt / 10 s**	**Current work**
UCC, Cork, Ireland	462	4 ppt / 57 s	Venables et al., 2006
UCC, Jülich, Germany**	1800 ± 20	0.5-2 ppt/5 s	(Dorn et al., 2013)
LPCA, Wimereux, France	2000	7.9 ppt / 1 min	Wu et al., 2014

*Deff is the effective length of the cavity, calculated by taking into account the dilution generated by the mirror protective flush
**UCC's IBBCEAS was used on SAPHIR chamber during an intercomparison campaign.

In order to evaluate if our detection limit can be improved by increasing the integration time, the Allan variance has been calculated for various integration times during an experiment in which NO_2 concentration was monitored. The NO_2 mixing ratio was approximatively 1300 ppb. The Allan variance σ_A^2 is given by the equation:

$$\sigma_A^2 = \frac{1}{2(M-1)} \sum_{i=1}^{M-1} [x_{i+1}(t_{av}) - x_i(t_{av})]^2 \qquad \text{(Eq.5)}$$

with M the number of measurements, t_{av} the integration time and x the concentration of NO_2 measured. In this experiment, 30 000 measurements of 2 seconds have been performed and the Allan variance was then calculated for various integration times ranging between 2 and 4096 seconds. The standard deviation of Allan, defined as the square root of the Allan variation provides an indication of the instrument stability in time. It is plotted as a function of the integration time in Fig. 5**Erreur ! Source du renvoi introuvable.**. For very short integration time (few seconds) the Allan deviation is very high due to the white noise of the instrument. The Allan deviation decreases with increasing integration time until 100 seconds. For longer integration times, the deviation increases with increasing integration time. Nevertheless, the deviation is low, showing that the instrument is very stable. Due to this stability, we expect that the detection limits calculated before can be improved by increasing integration time. From this test, it can be also concluded that the optimal integration time is around 100 seconds.
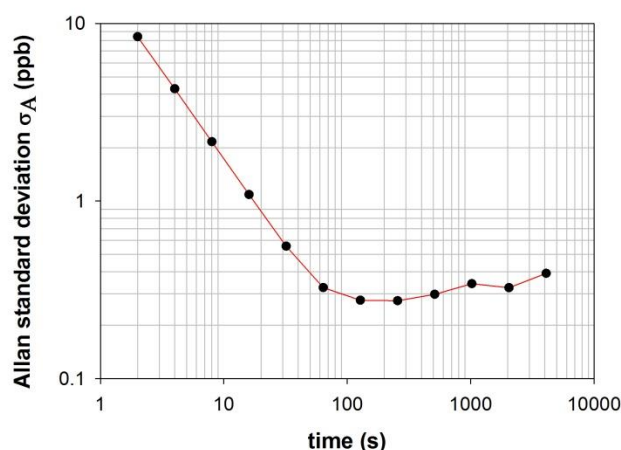
Figure 5: Allan variance vs. integration time calculated for the IBBCEAS technique

The high stability of the Allan deviation after 100 s also suggests that the stability of the optical device is optimal to perform measurements without recording a new $I_0(\lambda)$ for at least 4096 s, in agreement with the result of the test

presented in section 3.2. In conclusion, the good stability of the optical device complies with the constraint of
270 experiments in simulation chamber where $I_0(\lambda)$ can only be recorded at the beginning of the experiment.

3.4. Determination of the uncertainty

Considering Eq.1 and Eq. 2, the overall relative error on NO_3 concentration can be considered as the square root
of the sum of the square relative errors, the reflectivity $R(\lambda)$ and the NO_3 absorption cross sections. In case of the
use of the nitrogen flush, the uncertainty on d_{eff} has to be also taken into account (8 %, see Sect. 2). Considering
275 Eq. 3, the uncertainty on $R(\lambda)$ should include the uncertainty on NO_2 concentration measured by FTIR estimated
to be 8 % as well as the uncertainty on NO_2 absorption cross sections. The uncertainties on NO_2 and NO_3 cross
sections are estimated to be 3 % in the spectral range of interest (Vandaele et al. 1997 and Orphal, Fellows and
Flaud, 2003). However, the uncertainty generated by the data treatment Δfit, i.e. by the fit, which results mainly
from the noise in the spectra, should also be taken into account. Because the nitrate radical is an unstable species,
280 this uncertainty cannot be estimated by calculating the standard deviation on its concentrations measured for a
long period of monitoring. It was therefore estimated by considering the noise of a NO_3 concentration time profile
and has been found to be ~ 3ppt for 10 seconds of integration time. The overall absolute error on NO_3 concentration
is then expressed by the following formula:

$$\Delta N_{NO_3} = \sqrt{\left(\left(\frac{\Delta\sigma_{NO_2}(\lambda)}{\sigma_{NO_2}(\lambda)}\right)^2 + \left(\frac{\Delta N_{NO_2,refl}}{N_{NO_2,refl}}\right)^2 + \left(\frac{\Delta\sigma_{NO_3}}{\sigma_{NO_3}}\right)^2\right)} \times N_{NO_3} + \Delta fit \qquad \text{(Eq. 6)}$$

285 where $\frac{\Delta\sigma_{NO_2}(\lambda)}{\sigma_{NO_2}(\lambda)}, \frac{\Delta N_{NO_2,refl}}{N_{NO_2,refl}}, \frac{\Delta\sigma_{NO_3}}{\sigma_{NO_3}}$ are relative uncertainties on NO_2 cross sections, NO_2 concentration used for the
reflectivity measurement, NO_3 cross sections respectively and N_{NO_3} the concentration of NO_3. For 10 seconds of
integration time, the uncertainty is thus 9 % with an absolute part of 3 ppt.

4. Intercomparison study

After having defined the optimal operation conditions of the IBBCEAS, the technique has been validated thanks
290 to an intercomparison with another instrument. During a dedicated experiment, NO_3 and NO_2 concentrations were
measured by the IBBCEAS technique while NO_2 and N_2O_5 were monitored by *in situ* FTIR. The chamber was
first filled with dry synthetic air (RH < 1%) at atmospheric pressure and $I_0(\lambda)$ spectra were recorded for both FTIR
and IBBCEAS. Several hundred of ppb of NO_2 (Air Liquide N20, purity>99 %, H_2O<3000 ppm) were then
introduced into the chamber and IBBCEAS spectra were recorded in order to determine the mirrors reflectivity
295 $R(\lambda)$ (see Sect. 3.2). NO_3 radicals were then formed *in situ*, using thermal dissociation of N_2O_5 (R. (1)), which was
synthesized in a vacuum line following the reaction between O_3 and NO_2 (R. (2) and R. (3)). This protocol was
adapted from (Atkinson et al., 1984; Schott and Davidson, 1958) and is detailed in Picquet-Varrault et al., 2009.

$N_2O_5 + M \leftrightarrows NO_3 + NO_2 + M$ (R. 1)

$O_3 + NO_2 \rightarrow NO_3 + O_2$ (R. 2)

300 $NO_3 + NO_2 + M \rightarrow N_2O_5 + M$ (R. 3)

Then, by considering the following equilibrium:

$NO_2 + NO_3 + M \rightarrow N_2O_5 + M \ (k_1)$ (R. 4)

$N_2O_5 + M \rightarrow NO_2 + NO_3 + M \; (k_2)$ (R. 5)

And by assuming that this equilibrium is reached, NO_3 concentration can be deduced from NO_2 and N_2O_5 concentrations measured by FTIR. This hypothesis appears justified as no other reactive species has been introduced into the chamber and may thus disturb the equilibrium. The equilibrium constant ($K = k_1/k_2$) is well known and has been shown to highly depend on temperature and pressure (Atkinson et al., 2004). These two parameters were therefore precisely monitored during the experiment allowing calculating an equilibrium constant of 2.17×10^{-11} cm^3.molecule^{-1} at 298K and at 1030 mbar, using IUPAC database parameters (Atkinson et al., 2004). IBBCEAS spectra were recorded every 30 seconds while FTIR ones were recorded every 2 minutes. The integrated band intensities used to quantify NO_2 and N_2O_5 with FTIR were: IBI_{NO2} (1530-1680 cm^{-1}) = (5.6 ± 0.2) $\times 10^{-17}$ cm molecule^{-1} and IBI_{N2O5} (1200-1285 cm^{-1}) = (4.05 ± 0.4) $\times 10^{-17}$ cm molecule^{-1} (base e). The correlation plots between FTIR and IBBCEAS for NO_3 and NO_2 measurements are shown in Fig. 6**Erreur ! Source du renvoi introuvable.**. NO_2 concentrations measured by the two techniques are in very good agreement (the maximum difference between the two techniques is 6 %), with a slope of 1.0 ± 0.2. Here, the overall uncertainty was calculated as the sum of the statistical error on the slope (twice the standard deviation, 4 %) and systematic errors on FTIR (i.e. on IBI_{NO2}, 4 %) and IBBCEAS measurements (which includes uncertainties on NO_2 cross sections and on the mirrors reflectivity, 9%). The intercept of the linear regression (b = 15.0 ppb) is not significantly different from zero as it is lower than its uncertainty calculated as twice the standard deviation (Δb = 25.1 ppb). For NO_3 radical, the concentrations obtained by the two techniques are also in good agreement for the whole range of concentrations, from few ppt to several hundred ppt. The slope of the NO_3 correlation plot is 1.1 ± 0.3 suggesting a bias of 10 % between the two techniques. The error is calculated with the same method as for NO_2. However, this difference is not significant in regards to the uncertainties which are represented by the black dashed lines. For FTIR measurement, the uncertainties are calculated being the error on NO_2 and N_2O_5 measurement and on the equilibrium constant (21 %). The calculation for uncertainty on NO_3 IBBCEAS measurement is presented in section 3.4. The intercept appears to be very low (around 3 ppt).
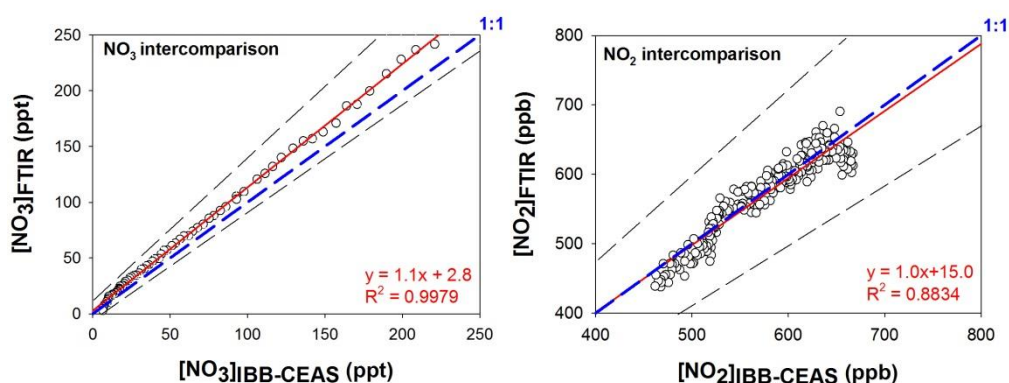
Figure 6 : Correlation between FTIR and IBBCEAS measurements for NO₃ (left graph) and NO₂ (right graph). Uncertainties are shown by dashed straight lines. Blue dashed lines show the 1:1 ratio.

In conclusion, the IBBCEAS exhibits very good agreement with the FTIR, for both NO_3 and NO_2 monitoring, with good sensitivity. This agreement is very satisfactory considering the fact that the IBBCEAS samples across the reactor width while the FTIR provides an integrated measurement on the whole reactor length. Finally, the intercomparison experiment shows that an eventual loss due to photolysis of NO_3 by the beam is not significant

because it would have led to lower concentrations measured by the IBBCEAS than by the FTIR. In addition, for wavelength longer than 640 nm, which is the case here, Johnston et al., 1996 have shown that photolysis quantum yield is close to 0. It is thus expected that the photolysis of NO_3 in the used wavelength range is not occuring. Furthermore even though NO_3 was slightly subject to photolysis locally, the volume enlightened by the probe beam is very small in comparison to the overall volume of the chamber ($< 0.04\%$) and the homogenization system allowed a mixing with the rest of the volume."

5. Kinetic study: NO_3 + *trans*-2-butene

The last step of the validation consisted in a kinetic experiment in order to assess the potential of the technique for kinetic studies: the IBBCEAS has been used to measure the rate constant of a well-known reaction: *trans*-2-butene + NO_3. This reaction has been chosen as it has been intensively studied in the literature. Six absolute rate determinations (Benter et al., 1992; Berndt et al., 1998; Dlugokencky and Howard, 1989; Kasyutich et al., 2002; Ravishankara and Mauldin, 1985; Rudich et al., 1996) and two relative ones (Atkinson et al., 1984; Japar and Niki, 1975) have been published leading to a recommendation by IUPAC (Atkinson et al., 2006). This reaction is also particularly interesting because it does not produce SOA. This will allow us to test the performances of the instrument for monitoring NO_3 concentrations with a high time resolution and to validate our kinetic determination by comparison with previous ones.

The rate constant was determined using the absolute rate technique and by measuring the consumption of *trans*-2-butene due to its reaction with NO_3. Because no other oxidant was present in the mixture, it was therefore assumed that *trans*-2-butene is consumed only by reaction with nitrate radical:

$$trans\text{-}2\text{-}butene + NO_3 \rightarrow Products \ (k_{trans\text{-}2\text{-}butene}) \tag{R. 6}$$

For this reaction, kinetic equation can be established as:

$$\frac{-d[trans\text{-}2\text{-}butene]}{dt} = k_{trans-2-butene}[NO_3][trans\text{-}2\text{-}butene] \tag{Eq. 7}$$

By making the hypothesis of small variations of time and [*trans*-2-butene], this relationship can be approximated to:

$$-\Delta[trans\text{-}2\text{-}butene] = k_{trans-2-butene}[NO_3][trans\text{-}2\text{-}butene]\Delta t \tag{Eq. 8}$$

Where $\Delta[trans\text{-}2\text{-}butene]$ corresponds to the consumption of *trans*-2-butene during the time interval Δt and [*trans*-2-butene] and [NO_3] are averaged concentrations measured during this period. By plotting $-\Delta$[*trans*-2-butene] vs. the product [*trans*-2-butene][NO_3]Δt, a straight line with the slope corresponding to $k_{trans\text{-}2\text{-}butene}$ is obtained. It is important to notice that because this absolute kinetic method consists of measuring the decay of *trans*-2-butene for a known concentration of NO_3, and not the decay of NO_3 radicals for a known concentration of the VOC, it is not affected by NO_3 additional loss processes (e.g. wall losses, reactions with NO_2 or with peroxy radicals). Only additional losses of the VOC would lead to an overestimation of the rate constant. So, it was checked prior to the experiments (i.e. before in the injection of N_2O_5) that no significant loss of the VOC was observed in the timescale of the experiment (see below).

Six kinetic experiments have been conducted in the dark, at room temperature (292 - 294 K) and atmospheric pressure in synthetic air. The initial conditions of reactants (*trans*-2-butene, N_2O_5, NO_2) are listed in Table 2**Erreur ! Source du renvoi introuvable.**. The reflectivity was measured prior to each experiment by introducing NO_2 into the chamber. When present, NO_2 initial concentrations were used also to slow down the reaction by shifting the N_2O_5 equilibrium. *Trans*-2-butene (Air Liquide, purity>99 %) was then introduced and it was checked that no significant loss was observed in the timescale of the experiment. Nitrate radicals were generated into the simulation chamber from the thermal decomposition of dinitrogen pentoxide. N_2O_5 was stepwise injected in order to assure a consumption of *trans*-2-butene in a proper timescale to satisfactory monitor the reactants. Time resolved concentrations of *trans*-2-butene, NO_2 and N_2O_5 were monitored from their infrared absorption spectra every 2 minutes. The integrated band intensity used to quantify the VOC is $IBI_{trans\text{-}2\text{-}butene}$ (870-1100 cm^{-1}) = (2.8 ± 0.3) × 10^{-18} cm molecule^{-1} (base e, measured by previous internal work). NO_3 was monitored with the IBBCEAS technique with an acquisition time of 30 seconds.

Table 2 : Injected mixing ratios for the kinetic study of the reaction *trans*-2-butene + NO₃

Experiment	[NO₂]₀ (ppb)	[N₂O₅] (ppb) × number of injections	[*trans*-2-butene]₀ (ppb)
1	/	2500	1920
2	/	300 × 2 ; 150 × 2	750
3	920	1000 × 3	990
4	950	1500 × 2	1110
5	750	300 × 3	1110
6	/	300 × 3	1030

Figure 7**Erreur ! Source du renvoi introuvable.** shows time profiles of reactants during a typical experiment. At the moment when N_2O_5 is injected, a rapid decrease of *trans*-2-butene and NO_3 concentrations is observed together with a large production of NO_2 due to N_2O_5 decomposition.
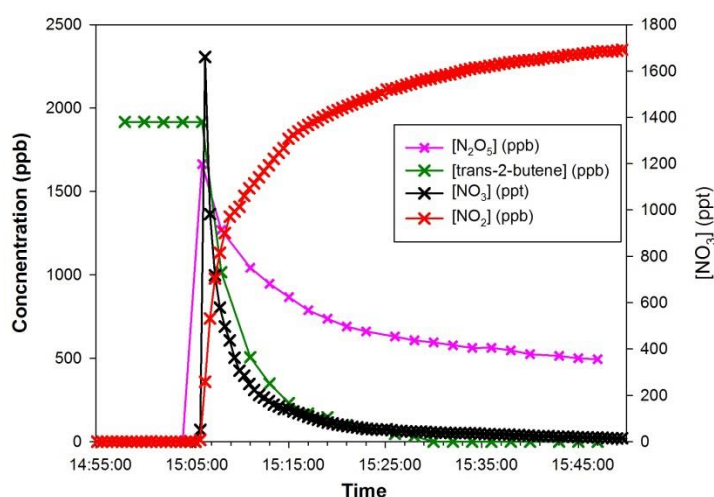
Figure 7 : Concentrations of *trans*-2-butene and NO₂ measured by FTIR (left axis) and NO₃ measured by IBBCEAS versus time (right axis) during experiment 1.

The kinetic plot ($-\Delta$[*trans*-2-butene] vs. the product [*trans*-2-butene]×[NO$_3$]×Δt) gathering data from all experiments is presented in Fig. 8**Erreur ! Source du renvoi introuvable.**. The uncertainty on each experimental point was calculated as the sum of the relative uncertainties on [*trans*-2-butene] and [NO$_3$] for the abscissa scale (the uncertainty on the time was considered to be negligible) and as twice the uncertainty on the [*trans*-2-butene] for the ordinate scale. From this figure, it can be observed that all experiments are in good agreement. In consequence, a linear regression was performed on all data points leading to a rate constant of $(4.13 \pm 0.78) \times 10^{-13}$ cm^3 molecule^{-1} s^{-1}. The uncertainty on the rate constant was estimated as the sum of the relative uncertainties on NO$_3$ concentrations and twice the standard deviation on the linear regression. The obtained rate constant has been compared to the values from previous determinations and to the value recommended by IUPAC in Table 3.
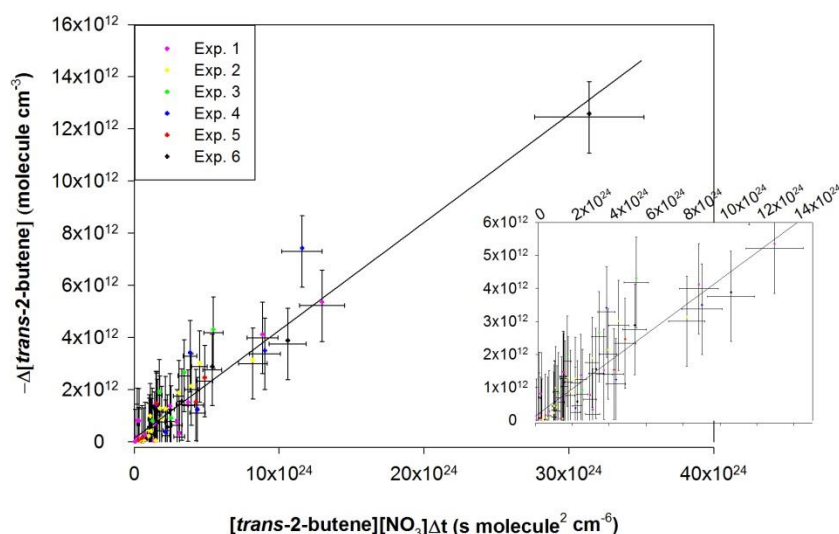
Figure 8 : Absolute kinetic plot for the reaction of *trans*-2-butene with NO$_3$ radical, showing the loss of trans-2-butene vs. [VOC]×[NO$_3$]×Δt. To the right, a zoom on the points close to the origin.

This new determination appears to be in very good agreement with the IUPAC recommendation and with previous absolute determinations, within the uncertainty. However this work does not agree with the two relative determinations which are up to 45 % lower than our determination. Nevertheless, these two values are in disagreement with all of the previous absolute determinations. These relative rate determinations are relative to the equilibrium constant K ($N_2O_5 + M \leftrightarrows NO_2 + NO_3$). A possible explanation to this disagreement would be that NO$_3$ concentration is overestimated because it was considered that the equilibrium is reached. However, the reaction with *trans*-2-butene is fast enough to significantly disturb the equilibrium and prevent it to be established. An overestimation of NO$_3$ concentrations would hence lead to an underestimation of the rate constant.

Table 3 : Comparison of the rate constant obtained for the reaction of *trans*-2-butene with NO$_3$ with previous determinations.

k (cm^3 molecule^{-1} s^{-1})	T (K)	Technique*	Reference
(4.13 ± 0.78) × 10^{-13}	**293**	**(N$_2$O$_5$/CEAS)**	**This study**
(3.90 ± 0.78) × 10^{-13} (Δlogk = ± 0.08)	298	recommendation	IUPAC
(3.78 ± 0.17) × 10^{-13}	298	(AR/CEAS)	(Kasyutich et al., 2002)
(3.74 ± 0.45) × 10^{-13}	298	(AR/LIF)	(Berndt et al., 1998)
(4.06 ± 0.36) × 10^{-13}	298	(AR/LIF)	(Rudich et al., 1996)
(3.88 ± 0.30) × 10^{-13}	298	(AR/MS)	(Benter et al., 1992)
(3.96 ± 0.48) × 10^{-13}	298	(AR/LIF)	(Dlugokencky and Howard, 1989)
(3.78 ± 0.17) × 10^{-13}	298	(AR/LIF)	(Ravishankara and Mauldin, 1985)
(3.09 ± 0.27) × 10^{-13}	298	(RR**)	(Atkinson et al., 1984)
(2.31 ± 0.17) × 10^{-13}	300	(RR**)	(Japar and Niki, 1975)

*Indicates kinetic method (AR = absolute rate, RR = relative rate) and NO$_3$ measurement technique: CEAS, LIF (Laser-Induced Fluorescence) or MS (mass spectrometry) used

415 ** Relative rate determinations are relative to the equilibrium constant $K\ (N_2O_5\ +\ M \leftrightarrows NO_2 + NO_3 + M)$.

In conclusion, this agreement shows that the determination made with the IBBCEAS technique presented in this paper is correct, allowing reliable measurement of NO$_3$ at low concentration with good sensitivity and time resolution. This technique is now operational for application to other absolute kinetic studies.

420 **6. Conclusions**

An IBBCEAS technique has been developed and coupled to the CSA simulation chamber for the *in situ* measurement of NO$_3$ radicals at the ppt level. This instrument allows also monitoring NO$_2$ in the ppb range. Thanks to various tests, the instrument has been carefully characterized in order to identify potential bias and to define the optimal operation conditions. The performance of the instrument in terms of detection limit and uncertainties were

425 also determined. The instrument exhibits very good detection limit for NO$_3$ radicals (6 ppt) for 10 seconds of integration time. This detection limit fully complies with our needs for kinetic applications.

The instrument was also validated thanks to an intercomparison experiment with the *in situ* FTIR technique. With this technique, NO$_3$ concentration was indirectly obtained by monitoring NO$_2$ and N$_2$O$_5$ concentrations and by using the well-known equilibrium constant $K\ (N_2O_5\ +\ M \leftrightarrows NO_2 + NO_3)$. The concentrations measured by the

430 two techniques were shown to be in very good agreement (better than 10%) for both NO$_3$ and NO$_2$, over a ride range of concentrations: from ppt to ppb range for NO$_3$ radical and from ppb to hundreds of ppb for NO$_2$.

Finally, this technique was used for the absolute rate determination of a well-documented reaction, *trans*-2-butene+ NO$_3$. The value of (4.13 ± 0.45) × 10^{-13} cm^3 molecule^{-1} s^{-1} found in this study is in very good agreement with the previous absolute determinations. Moreover, the good sensitivity and the good time resolution represent excellent

435 performances allowing the use of this technique for monitoring NO$_3$ radicals when involved in fast reactions.

The IBBCEAS technique is now operational and will be used in further works, particularly to monitor NO$_3$ concentrations for absolute rate determinations of fast reactions of volatile organic compounds with NO$_3$ radicals.

Data availability. Rate constant for the NO$_3$ oxidation of *trans*-2-butene is available Table 3. It is also available through the Library of Advanced Data Products (LADP) of the EUROCHAMP data center (https://data.eurochamp.org/data-access/ gas phase-rate-constants/, last access: 25 March 2020, Fouqueau et al., 2020a). Simulation chamber experiments which were used to retrieve these parameters and for the intercomparison are available through the Database of Atmospheric Simulation Chamber Studies (DASCS) of the EUROCHAMP data center (https://data.eurochamp.org/data-access/chamber-experiments/, last access: 25 March 2020, Fouqueau et al., 2020b).

Author contributions. MCi, BPV and AF designed the IBBCEAS technique with the help of GM and DR. AF installed and did characterization experiments with the technical support of XL (optical development), MCa and EP (experiments), PZ and GS (data treatment). MCi, BPV and AF wrote the article and AF was responsible for the final version. All coauthors revised the content of the original manuscript and approved the final version of the paper.

Competing interests. The authors declare that they have no conflict of interest.

Financial support. This work was supported by the French national programme LEFE/INSU and by the European Commission's Seventh Framework Programme (EUROCHAMP-2; grant no. 228335), H2020 Research Infrastructures (EUROCHAMP-2020; grant no. 730997).

References

Atkinson, R.: Atmospheric chemistry of VOCs and NOx, Atmos Env., 34, 2063–2101, 2000.

Atkinson, R., Plum, C. N., Carter, W. P. L., Winer, A. M. and Pitts, J. N.: Rate constants for the gas-phase reactions of nitrate radicals with a series of organics in air at 298 .+-. 1 K, J. Phys. Chem., 88(6), 1210–1215, doi:10.1021/j150650a039, 1984.

Atkinson, R., Baulch, D. L., Cox, R. A., J. N., H., Hynes, R. G., Jenkin, M. E., Rossi, M. J. and Troe, J.: Evaluated kinetic and photochemical data for atmospheric chemistry: Volume I - gas phase reactions of Ox, HOx, NOx and SOx species, Atmos Chem Phys, 4, 1461–1738, 2004.

Atkinson, R., Baulch, D. L., Cox, R. A., Crowley, J. N., Hampson, R. F., Hynes, R. G., Jenkin, M. E., Rossi, M. J., Troe, J. and IUPAC Subcommittee: Evaluated kinetic and photochemical data for atmospheric chemistry: Volume II – gas phase reactions of organic species, Atmos Chem Phys, 6, 3625–4055, 2006.

Ball, S. M., Langridge, J. M. and Jones, R. L.: Broadband Cavity Enhanced Absorption Spectroscopy using Light Emitting Diodes, Chem Phys Lett, 398, 68–74, doi:10.1016/j.cplett.2004.08.144, 2004.

Benter, Th., Becker, E., Wille, U., Rahman, M. M. and Schindler, R. N.: The Determination of Rate Constants for the Reactions of Some Alkenes with the NO3 Radical, Berichte Bunsenges. Für Phys. Chem., 96(6), 769–775, doi:10.1002/bbpc.19920960607, 1992.

Berndt, T., Kind, I. and Karbach, H.-J.: Kinetics of the Gas-Phase Reaction of NO3 Radicals with 1-Butene, trans-Butene, 2-Methyl-2-butene and 2,3-Dimethyl-2-butene Using LIF Detection, Berichte Bunsenges. Für Phys. Chem., 102(10), 1486–1491, doi:10.1002/bbpc.199800017, 1998.

Bitter, M., Ball, S. M., Povey, I. M. and Jones, R. L.: A broadband cavity ringdown spectrometer for in-situ measurements of atmospheric trace gases, Atmos Chem Phys, 5, 2547–2560, doi:doi.org/10.5194/acp-5-2547-2005, 2005.

480   Brown, S. S. and Stutz, J.: Nighttime radical observations and chemistry, Chem. Soc. Rev., 41(19), 6405–6447, doi:10.1039/C2CS35181A, 2012.

Calvert, J. G., Orlando, J. J., Stockwell, W. R. and Wallington, T. J.: The Mechanisms of Reactions Influencing Atmospheric Ozone, Oxford University Press, New York., 2015.

Dlugokencky, E. J. and Howard, C. J.: Studies of nitrate radical reactions with some atmospheric organic
485   compounds at low pressures, J Phys Chem, 93, 1091–1096, 1989.

Dorn, H.-P., Apodaca, R. L., Ball, S. M., Brauers, T., Brown, S. S., Crowley, J. N., Dubé, W. P., Fuchs, H., Häseler, R., Heitmann, U., Jones, R. L., Kiendler-Scharr, A., Labazan, I., Langridge, J. M., Meinen, J., Mentel, T. F., Platt, U., Pöhler, D., Rohrer, F., Ruth, A. A., Schlosser, E., Schuster, G., Shillings, A. J. L., Simpson, W. R., Thieser, J., Tillmann, R., Varma, R., Venables, D. S. and Wahner, A.: Intercomparison of NO3 radical
490   detection instruments in the atmosphere simulation chamber SAPHIR, Atmos Meas Tech, 6(5), 1111–1140, doi:10.5194/amt-6-1111-2013, 2013.

Engel, R., Berden, G., Peeters, R. and Meijer, G.: Cavity enhanced absorption and cavity enhanced magnetic rotation spectroscopy, Rev. Sci. Instrum., 69, 3763, 1998.

Fuchs, H., Ball, S. M., Bohn, B., Brauers, T., Cohen, R. C., Dorn, H.-P., Dubé, W. P., Fry, J. L., Häseler, R.,
495   Heitmann, U., Jones, R. L., Kleffman, J., Mentel, T. F., Müsgen, P., Rohrer, F., Rollins, A. W., Ruth, A. A., Kiendler-Scharr, A., Schlosser, E., Shillings, A. J. L., Tillmann, R., Varma, R., Venables, D. S., Villena Tapia, G., Wahner, A., Wegener, R., Wooldridge, P. J. and Brown, S. S.: Intercomparison of measurements of NO2 concentrations in the atmosphere simulation chamber SAPHIR during the NO3Comp campaign, Atmos Meas Tech, 3, 21–37, doi:10.5194/amt-3-21-2010, 2010.

500   Ihaka, R. and Gentleman, R.: R: A language for data analysis and graphics, J. Comput. Graph. Stat., 5(3), 299–314, 1996.

Japar, S. M. and Niki, H.: Gas-phase reactions of the nitrate radical with olefins, J Phys Chem, 79(16), 1629–1632, 1975.

Johnston, H. S., Davis, H. F. and Lee, Y. T.: NO3 Photolysis Product Channels: Quantum Yields from Observed
505   Energy Thresholds, J. Phys. Chem., 100(12), 4713–4723, doi:10.1021/jp952692x, 1996.

Kasyutich, V. L. ;, Canosa-Mas, C. E. ;, Pfrang, C. ;, Vaughan, S. and Wayne, R. P.: Off-axis continuous-wave cavity-enhanced absorption spectroscopy of narrow-band and broadband absorbers using red diode lasers, Appl. Phys. B Lasers Opt., 75, 2002.

Kennedy, O. J., Ouyang, B., Langridge, J. M., Daniels, M. J. S., Bauguitte, S., Freshwater, R., McLeod, M. W.,
510   Ironmonger, C., Sendall, J., Norris, O., Nightingale, R., Ball, S. M. and Jones, R. L.: An aircraft based three channel broadband cavity enhanced absorption spectrometer for simultaneous measurements of NO3, N2O5 and NO2, Atmos Meas Tech, 4(9), 1759–1776, doi:10.5194/amt-4-1759-2011, 2011.

Kerdouci, J., Picquet-Varrault, B., Durand-Jolibois, R., Gaimoz, C. and Doussin, J.-F.: An experimental study of the gas-phase reactions of NO3 radicals with a series of unsaturated aldehydes: trans-2-hexenal, trans-2-heptenal
515   and trans-2-octenal, J Phys Chem A, 116, 10135–1014, 2012.

Langridge, J. M., Ball, S. M., Shillings, A. J. L. and Jones, R. L.: A broadband absorption spectrometer using light emitting diodes for ultrasensitive, in situ trace gas detection, Rev. Sci. Instrum., 79(12), 123110, doi:10.1063/1.3046282, 2008.

Matsumoto, J., Kosugi, N., Imai, H. and Kajii, Y.: Development of a measurement system for nitrate radical and
520   dinitrogen pentoxide using a thermal conversion/laser-induced fluorescence technique, Rev. Sci. Instrum., 76, 064101, doi:10.1063/1.1927098, 2005a.

Matsumoto, J., Imai, H., Kosugi, N. and Kajii, Y.: In situ measurement of N2O5 in the urban atmosphere by thermal decomposition/laser-induced fluorescence technique, Atmos Env., 39(36), 6802–6811, doi:10.1016/j.atmosenv.2005.07.055, 2005b.

525 Matsumoto, J., Imai, H., Kosugi, N. and Kajii, Y.: Methods for preparing standard nitrate radical (NO 3) gas to calibrate the LIF-based instrument for measurements in the atmosphere, Chem Lett, 34(9), 1214–1215, doi:10.1246/cl.2005.1214, 2005c.

Naudet, J. P., Huguenin, D., Rigaud, P. and Cariolle, D.: Stratospheric observations of NO3 and its experimental and theoretical distribution between 20 and 40 km, Planet. Space Sci., 29(6), 707–712, doi:10.1016/0032-
530 0633(81)90118-5, 1981.

Ng, N. L., Brown, S. S., Archibald, A. T., Atlas, E., Cohen, R. C., Crowley, J. N., Day, D. A., Donahue, N. M., Fry, J. L., Fuchs, H., Griffin, R. J., Guzman, M. I., Herrmann, H., Hodzic, A., Iinuma, Y., Jimenez, J. L., Kiendler-Scharr, A., Lee, B. H., Luecken, D. J., Mao, J., McLaren, R., Mutzel, A., Osthoff, H. D., Ouyang, B., Picquet-Varrault, B., Platt, U., Pye, H. O. T., Rudich, Y., Schwantes, R. H., Shiraiwa, M., Stutz, J., Thornton, J.
535 A., Tilgner, A., Williams, B. J. and Zaveri, R. A.: Nitrate radicals and biogenic volatile organic compounds: oxidation, mechanisms, and organic aerosol, Atmos Chem Phys, 2103–2162, 2017.

Noxon, J. F., Norton, R. B. and Henderson, W. R.: Observation of atmospheric NO3, Geophys. Res. Lett., 5, 675–678, 1978.

Noxon, J. F., Norton, R. B. and Marovich, E.: NO3 in the troposphere, Geophys. Res. Lett., 7(2), 125–128,
540 doi:10.1029/GL007i002p00125, 1980.

Orphal, J., Fellows, C. E. and Flaud, P.-M.: The visible absorption spectrum of NO_3 measured by high-resolution Fourier transform spectroscopy, J Geophys Res, 108, 4077, 2003.

Picquet-Varrault, B. ;, Scarfogliero, M. ;, Ait Helal, W. ; and Doussin, J.-F. ; Reevaluation of the rate constant for the reaction propene + NO_3 by absolute rate determination, Int. J. Chem. Kinet., 41, 73–81, 2009.

545 Platt, U., Perner, D., Harris, G. W., Winer, A. M. and Pitts, J. N.: Observations of nitrous acid in an urban atmosphere by differential optical absorption, Nature, 285(5763), 312–314, doi:10.1038/285312a0, 1980.

Powell, M. J. D.: The BOBYQA algorithm for bound constrained optimization without derivatives., 2009.

Ravishankara, A. R. and Mauldin, R. L.: Absolute rate coefficient for the reaction of nitrogen trioxide (NO_3) with trans-2-butene, J Phys Chem, 89, 3144–3147, 1985.

550 Romanini, D., Kachanov, A. A., Sadeghi, N. and Stoeckel, F.: CW cavity ring down spectroscopy, Chem Phys Lett, 264(3–4), 316–322, doi:10.1016/S0009-2614(96)01351-6, 1997.

Rudich, Y., Talukdar, R. K., Fox, R. W. and Ravishankara, A. R.: Rate Coefficients for Reactions of NO_3 with a Few Olefins and Oxygenated Olefins, J Phys Chem, 100, 5374–5381, 1996.

Scarfogliero, M., Picquet-Varrault, B., Salce, J., Durand-Jolibois, R. and Doussin, J.-F.: Kinetic and Mechanistic
555 Study of the Gas-Phase Reactions of a Series of Vinyl Ethers with the Nitrate Radical, J Phys Chem A, 110, 11074–11081, 2006.

Schott, G. and Davidson, N.: Shock waves in chemical kinetics : The decomposition of N_2O_5 at high temperatures, J. Am. Chem. Soc., 80, 1841–1853, 1958.

Vandaele, A. C., Hermans, C., Simon, P. C., Carleer, M., Colin, R., Fally, S., Mérienne, M. F., Jenouvrier, A.
560 and Coquart, B.: Measurements of the NO2 absorption cross-section from 42000 cm-1 to 10000 cm-1 (238-1000 nm) at 220 K and 294 K, J. Quant. Spectrosc. Radiat. Transf., 171–184, 1997.

Varma, R., Ball, S. M., Brauers, T., Dorn, H.-P., Heitmann, U., Jones, R. L., Platt, U., Pöhler, D., Ruth, A. A., Shillings, A. J. L., Thieser, J., Wahner, A. and Venables, D. S.: Light extinction by secondary organic aerosol: an intercomparison of three broadband cavity spectrometers, Atmos Meas Tech, 6, 3115–3130, doi:10.5194/amt-
565 6-3115-2013, 2013.

Venables, D. S., Gherman, T., Orphal, J., Wenger, J. C. and Ruth, A. A.: High sensitivity in situ monitoring of NO3 in an atmospheric simulation chamber using incoherent broadband cavity-enhanced absorption spectroscopy, Environ. Sci. Technol., 40(21), 6758–6763, 2006.

570 Ventrillard-Courtillot, I., Sciamma O'Brien, E., Kassi, S., Méjean, G. and Romanini, D.: Incoherent Broad Band Cavity Enhanced Absorption Spectroscopy for simultaneous trace measurements of NO2 and NO3 with a LED source, Appl Phys B, 661–669, 2010.

Wayne, R. P., Barnes, I., Biggs, P., Burrows, J. P., Canosa-Mas, C. E., Hjorth, J., Le Bras, G., Moortgat, G. K., Perner, D., Poulet, G., Restelli, G. and Sidebottom, H.: The nitrate radical: Physics, chemistry, and the atmosphere, Atmos Env. Part A, 25, 1–203, 1991.

575 Wood, E. C., Wooldridge, P. J., Freese, J. H., Albrecht, T. and Cohen, R. C.: Prototype for In Situ Detection of Atmospheric NO3 and N2O5 via Laser-Induced Fluorescence, Env. Sci Technol, 37(24), 5732–5738, 2003.

Wu, T., Coeur-Tourneur, C., Dhont, G., Cassez, A., Fertein, E., He, X. and Chen, W.: Simultaneous monitoring of temporal profiles of NO3, NO2 and O3 by incoherent broadband cavity enhanced absorption spectroscopy for atmospheric applications, J. Quant. Spectrosc. Radiat. Transf., 133, 199–205, doi:10.1016/j.jqsrt.2013.08.002, 580 2014.